

## Cross sections for the dissociative electron attachment to ozone

S A Rangwala<sup>†</sup>, S V K Kumar<sup>†</sup>, E Krishnakumar<sup>†</sup> and N J Mason<sup>†‡</sup>

<sup>†</sup> Tata Institute of Fundamental Research, Homi Bhabha Road, Mumbai 400005, India

<sup>‡</sup> Department of Physics and Astronomy, University College London, Gower Street, London WC1E 6BT, UK

E-mail: sadiq@tifrc3.tifrc.res.in, svkk@tifrc4.tifrc.res.in,  
ekkmur@tifrc.res.in and nigel.mason@ucl.ac.uk

Received 18 January 1999

**Abstract.** The cross sections for the dissociative electron attachment (DEA) to ozone have been measured. Care has been taken to collect all the high kinetic energy fragments such that the present absolute DEA cross section measurements are believed to be the most accurate measurements made across the range from 0 to 10 eV for ozone. Our results have been interpreted with the help of both existing data in the literature and quantum chemical calculations performed on the neutral and negative-ion states of ozone.

### Introduction

Ozone ( $O_3$ ) is an important molecule due to both its environmental and technological relevance. Ozone is an unusual triatomic molecule, since it has weak bonding between the singly occupied  $\pi$ -orbitals on the terminal oxygen atoms. Hence ozone has both a low dissociation energy and many low-lying excited states. The above reasons have given a great impetus to the study and understanding of  $O_3$  and its role in the environment, motivating both experimental and theoretical investigations. The phenomenon of dissociative electron attachment (DEA) is an important tool for the investigation of the negative-ion resonances of molecules, providing insight into the structure and dynamics of both the parent molecule and the negative ion. In this paper, we report the absolute cross section measurements for DEA to ozone.

The status of earlier measurements for low-energy electron attachment and dissociative electron attachment to  $O_3$  may be summarized as follows. Stelman *et al* (1972) measured low-energy electron attachment to  $O_3$  using the swarm technique. Their estimates of the attachment cross sections were made from an analysis of rate coefficients in the energy range from 0.02 to 0.30 eV. Beam experiments performed by Curran (1961) reported the relative cross sections for  $O^-$  and  $O_2^-$  ion formation by DEA to  $O_3$ , over an incident electron energy range from 0.0 to  $\sim 3.0$  eV. A single peak was observed for both  $O^-$  and  $O_2^-$  ion yields with a maximum close to 1 eV. Allan *et al* (1996a) performed a detailed experimental study of the resonances formed by the collision of low-energy electrons with  $O_3$ . Their study focused on the elastic, vibrationally inelastic and DEA channels with incident electron energies up to 10 eV. Walker *et al* (1996) determined the relative intensities of the  $O^-$  and  $O_2^-$  ions produced in DEA to  $O_3$  in the energy range from 0 to 10 eV. The measurements by Curran, Allan *et al* and Walker *et al* are mutually consistent but relative in nature. The only absolute DEA measurement on  $O_3$  was reported by Skalny *et al* (1996). However, in contrast to the experiments of Allan *et al*

(1996a) and Walker *et al* (1996), they did not observe ion yields at electron energies higher than 3 eV. Therefore, there remains a need for a definitive measurement of the absolute cross section measurement of DEA to O<sub>3</sub>.

It is interesting to note that despite their importance, most of these measurements have only been made in the last three years. One of the major problems with making absolute measurements on O<sub>3</sub> is the fact that it is a highly reactive gas and readily degrades into O<sub>2</sub> as a function of time. This means that a very careful estimation of the concentration of O<sub>3</sub> in the mixture of O<sub>3</sub> and O<sub>2</sub> is vital to any measurement which attempts to measure absolute numbers. The experiment has to be controlled carefully as ozone induces potential drifts in the system, which must be corrected for. Also, since O<sub>3</sub> is a strong oxidizing agent, it attacks the electron gun filament causing frequent breakages. An additional problem is the elimination of all O-rings in those parts of the experiment where the O<sub>3</sub> concentrations are high as ozone reacts with those producing large quantities of CO and CO<sub>2</sub>. Hence, the measurement of the absolute cross sections for the DEA process in O<sub>3</sub> is difficult.

All of the above difficulties have been overcome in the current experiment allowing an accurate determination of absolute cross sections for the formation of the O<sup>-</sup> and O<sub>2</sub><sup>-</sup> ions. This experimental technique has been reliably established for the measurement of absolute, stable-ion, integrated cross sections, for electron impact ionization and dissociative attachment processes (Krishnakumar and Srivastava 1992, Krishnakumar and Nagesha 1992, Krishnakumar *et al* 1996, 1997) and also tested by remeasuring the DEA cross sections for O<sub>2</sub>. In the current experiment, it is also possible to change quickly from positive-ion detection to negative-ion detection, an advantage which is vital to the concentration measurement of O<sub>3</sub> in the interaction region.

### Experimental details

Our experimental arrangement is illustrated in figure 1. It shows a Pierce-type electron gun situated vertically above the interaction region (the intersection volume of the molecular and electron beams) and a Faraday cup placed below the interaction region, both of which are on the common axis of a pair of encircling, cylindrical, magnetic field coils used to collimate the electron beam. A multi-element time of flight (TOF) tube ending in a shielded channel electron multiplier is placed at right angles to the axis of the above arrangement. Perpendicular to the axis of the flight tube, symmetrically on both sides of the interaction region are a stainless steel pusher plate and a molybdenum puller mesh constituting the ion extraction arrangement. The target gas is introduced into the interaction region through a long, narrow capillary of 1.0 mm diameter, protruding through the pusher plate into the interaction region such that its tip is ~2.0 mm away from the interaction region.

The experimental method uses both a pulsed electron beam and a pulsed ion extraction voltage. The O<sub>3</sub> and O<sub>2</sub> mixture is leaked into the interaction region via the capillary forming an effusive beam. A capacitance manometer is placed just behind the capillary to measure the stagnation pressure of the gas mixture. The molecular beam is intersected by a pulsed electron beam (300 ns duration) in the interaction region producing positive and negative ions. Each pulse of ions is then swept into the flight tube by the application of a 200 V cm<sup>-1</sup>, 1 μs pulsed field applied to the pusher plate. The puller is held at ground potential throughout. The large extraction pulse used is effective in sweeping out all the ions from the interaction region, irrespective of fragment ion kinetic energy, into the multi-element flight tube, which is operated as an electrostatic lens assembly such that all the ions extracted are focused onto the detector. (Since the ions of interest are O<sup>-</sup> and O<sub>2</sub><sup>-</sup>, resulting in a mass to charge ratio difference of 16, the poor resolution of the mass spectrum, due to lensing, does not affect the measurement,

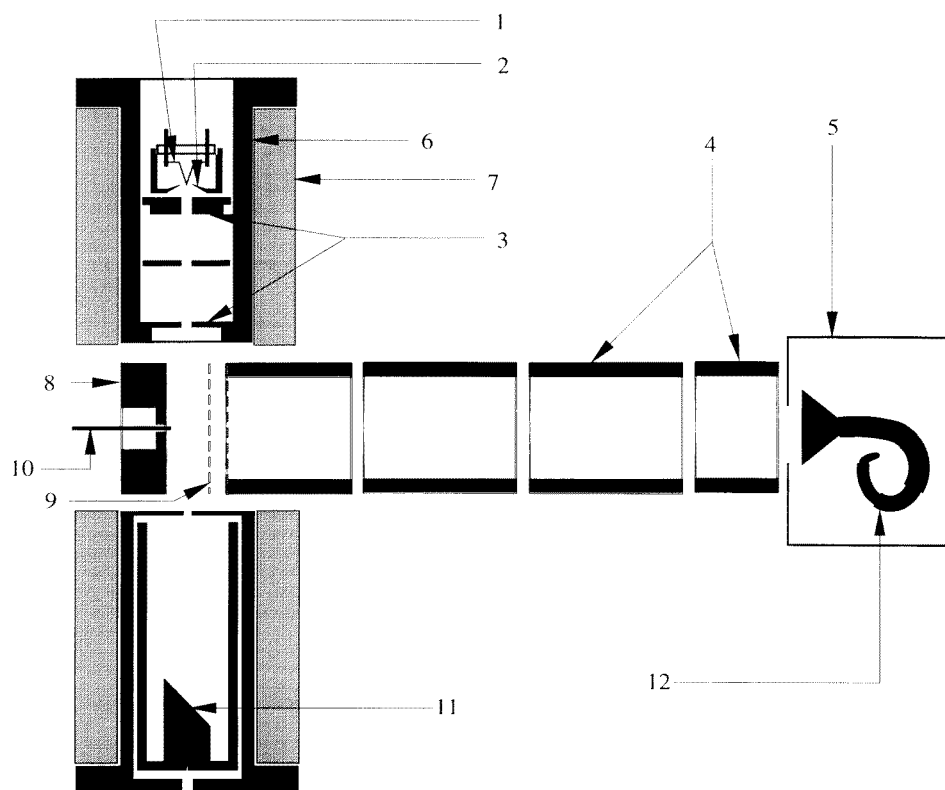


**Figure 1.** Schematic diagram of the experimental setup. The numbering represents (1): filament, (2): Pierce element, (3): gun electrodes, (4): flight tube elements, (5): channeltron housing, (6): electron gun housing, (7): magnetic field coil, (8): pusher electrode, (9): puller electrode, (10): capillary, (11): Faraday cup, (12): channel electron multiplier (channeltron).

as the ion peaks are non-overlapping.) The technique of pulsed electron beam and pulsed ion extraction, coupled with appropriate potentials on the flight tube elements, ensures the focusing of almost all the ions onto the detector. The success of this method in the collection of all the ion fragments, irrespective of their kinetic energies, has been addressed at length by Krishnakumar *et al* (1997). This was also tested in the present experiment by the measurement of the ratio of  $\text{H}_2^+$  (negligible kinetic energy) to  $\text{H}^+$  (very large kinetic energy) ions produced by electron impact of  $\text{H}_2$  at 100 eV and comparing it with reported values (Krishnakumar and Srivastava 1994, Van Zyl and Stephen 1994). A channel electron multiplier, operating in the pulse counting mode, is used for the detection of the ions. The signal pulses from the channeltron are extracted in the form of a voltage signal, processed through a pre-amplifier and then passed onto a constant fraction discriminator to act as a stop pulse of a time to amplitude converter (TAC). The start pulse for the TOF detection is derived from the master pulse generator used for pulsing the electron gun. The start and stop pulses are fed to the time to amplitude converter/single channel analyser (TAC/SCA) units, one for each ion of interest, and then to a pulse height analyser (PHA) for a mass spectrum or a multi-channel scalar (MCS) for the excitation function. The experiment is deliberately operated under conditions such that the rate of signal counts is under 10% of the trigger rate. This ensures that the effect of pile up discrimination, which occurs when two ion counts are detected for the same trigger pulse,

is minimized in the counting electronics.

The electron energy is controlled by the application of a bias on the filament tip of the electron gun. The energy resolution of the electron beam is estimated to be between 0.4 and 0.5 eV. This was performed by comparing with the reported data on known narrow resonances. The entire experiment is computer controlled. The electron gun bias supply can be ramped in programmed steps, for specified times, in order to obtain the relative ion formation cross sections as a function of incident electron energy. The computer interface (Kumar *et al* 1997) allows excitation functions of both  $O^-$  and  $O_2^-$  ions to be collected simultaneously as a function of electron energy. In addition, acquisition of all the experimental parameters, e.g. electron current and gas pressure, is performed on-line. These on-line measurements are very important in the normalization of our experimental data and help significantly in the reduction of errors in the relative and absolute cross sections.

The electron energy scale for the DEA cross sections is calibrated using the DEA peak energy values of the  $O_2$ , CO and  $CO_2$  molecules. In our experiment an error in the peak energies of  $\pm 0.1$  eV can be expected. The magnetic collimation of the electron beam provided almost constant beam current from approximately 0.7 eV onwards. However, since the electron current is seen to rise with increasing electron energy up to 0.7 eV, the ion counts were normalized to unit current.

Ozone was prepared by flowing oxygen through a silent electric discharge in a commercial ozonizer unit (Fischer Ozon 502). This unit produces a concentration of  $O_3$  between 1 and 2%. The concentration of  $O_3$ , in the resultant  $O_3$  and  $O_2$  mixture, was improved by passing this mixture through a silica-gel trap cooled to  $\sim 200$  K. This procedure allowed the ozone to be preferentially adsorbed on the surface of the gel. After trapping sufficient quantities, the residual  $O_2$  was pumped out leaving behind a reasonably pure sample of ozone. The trapped  $O_3$  was then desorbed from the silica gel and collected in a 5 l glass bulb. This bulb was then attached to the experimental chamber for experiments. The entire production and purification described above was performed using the University College London mobile ozonizer (Newson *et al* 1995).

The absolute cross sections were determined using the relative pressure technique (Krishnakumar *et al* 1997). This technique is used to place the cross sections on an absolute scale by comparing the relative intensities of the ionic species emerging from the molecule of interest with that of a species of known cross section collected under identical experimental conditions. The appropriate expression relating the two cross sections can be written as below, where the ion of interest is  $O^-$  from  $O_3$  and the calibration is against the  $O^-$  ion from  $O_2$ .

$$\sigma_{O^-/O_3} = \sigma_{O^-/O_2} \frac{N_{O^-/O_3}}{N_{O^-/O_2}} \frac{P_{O_2}}{P_{O_3+O_2}} \frac{K_{O_2}}{K_{O_3}} \frac{I_{O_2}}{I_{O_3}} \frac{1}{C_{O_3}}. \quad (1)$$

In the above expression,  $\sigma$  represents the cross section for the subscripted ion,  $N$  the number of recorded counts,  $P$  the pressure of the gas being flowed into the chamber measured by the MKS Baratron just behind the capillary,  $K$  the transmission coefficient for the detection of ions formed from different gases,  $I$  the measured electron current in the Faraday cup using a Keithley electrometer and  $C$  the concentration of  $O_3$  in the mixture of  $O_2$  and  $O_3$  introduced in the interaction region.

With pure gaseous targets, the last term would not be present but since in our experiment we produce a mixture of  $O_2$  and  $O_3$ , we need to experimentally measure the percentage of  $O_3$  pressure in the mixture to determine the cross section. The concentration of ozone was measured in the interaction region by changing to positive-ion detection mode before and after every cross section measurement of the negative ion. Measurement of the positive-ion counts of  $O_3^+$  and  $O_2^+$  produced by dissociative ionization of ozone at 100 eV in conjunction with

the cross section measurements of  $O^+$  and  $O_2^+$  ions from  $O_2$  at 100 eV of Krishnakumar and Srivastava (1992) and that of  $O^+$ ,  $O_2^+$  and  $O_3^+$  ions from  $O_3$  at 100 eV by Newson *et al* (1995) allows the ozone concentration in the experimental interaction region to be determined by;

$$C_{O_3} = \frac{1.814 \times N_{O_3^+}}{N_{O_2^+} + (0.884 \times N_{O_3^+})}. \quad (2)$$

Here  $N_{O_3^+}$  is the number of integrated  $O_3^+$  ion counts from  $O_3$  and  $N_{O_2^+}$  is the number of  $O_2^+$  ion counts from  $O_2$  and  $O_3$ , at 100 eV incident electron energy. The highest measured concentration was 55% at the interaction region. We estimate the purity of the  $O_3$  in the bulb to be between 70 and 80% and explain the decrease in the measured concentration as being due to the degradation of  $O_3$  during the transfer from the gas bulb to the interaction region.

### Estimation of errors

The error in our measurement of the absolute cross section is higher than for pure targets, primarily because it relies on three other cross section measurements as opposed to normally just one in pure gases. The cross sections are determined using the data of Rapp and Briglia (1965), for the formation of  $O^-$  from  $O_2$  with 10% one-sigma error, as the calibrator. The data of Krishnakumar and Srivastava (1992) for  $O^+$  from  $O_2$ , with 13% one-sigma error and that of Newson *et al* (1995) for  $O^+$  from  $O_3$ , with 15% one-sigma error were used for determining the concentration of  $O_3$  in the interaction region. Hence the inherent errors of these three measurements are incorporated in our measurement. Other uncertainties in our experiment are (a) the 2% uncertainty in the pressure measurement, (b) the 3% statistical error in counting, (c) the 2% error in the reproducibility of the excitation function, (d) the 2% error in the electron current measurement and (e) the 3% error in ion detection efficiency. The combined one-sigma error for our measurement is  $\pm 23\%$ . The error in the electron energy calibration is  $\pm 0.1$  eV. One source of systematic error at near-zero incident electron energy is the increase in the path length of the electrons due to their helical motion in the magnetic field, which results in larger than true cross sections (Kieffer and Dunn 1966). Rough estimates show that this may have a significant contribution only to energies below 0.5 eV. Therefore, the present results have not been corrected for this feature.

### Results and discussion

The DEA cross sections of  $O^-$  and  $O_2^-$  ions from  $O_3$  are plotted as a function of the incident electron energy in figure 2. The obvious observation from these excitation functions is that the  $O^-$  ion shows many more negative-ion resonances than the  $O_2^-$ . The features are summarized in table 1.

Our data is in good qualitative agreement with the data of Walker *et al* (1996). All the basic features seen in their experiment are reproduced in ours. The relative intensities of the ion peaks at different energies are also in reasonable agreement. The cross section measurements of Skalny *et al* (1996) report an ion signal only below 3 eV incident electron energy. Above 3 eV, Skalny *et al* did not observe the negative-ion signal observed in the present experiment and in those of Walker *et al* or Allan *et al* (1996a). This may be ascribed to Skalny *et al* being unable to detect fast  $O^-$  fragments. Skalny *et al* reported cross section values for the first DEA peaks of  $O^-$  at 1.35 eV as  $2.8 \times 10^{-17}$  cm<sup>2</sup> and for the corresponding  $O_2^-$  peak at 1.15 eV as  $1.8 \times 10^{-17}$  cm<sup>2</sup>. Their value for the  $O_2^-$  cross section is in very good agreement with our value of  $1.68 \times 10^{-17}$  cm<sup>2</sup>, the difference being about 7%, which is within the error of either measurement. Since our electron energy resolution is poor compared with that of

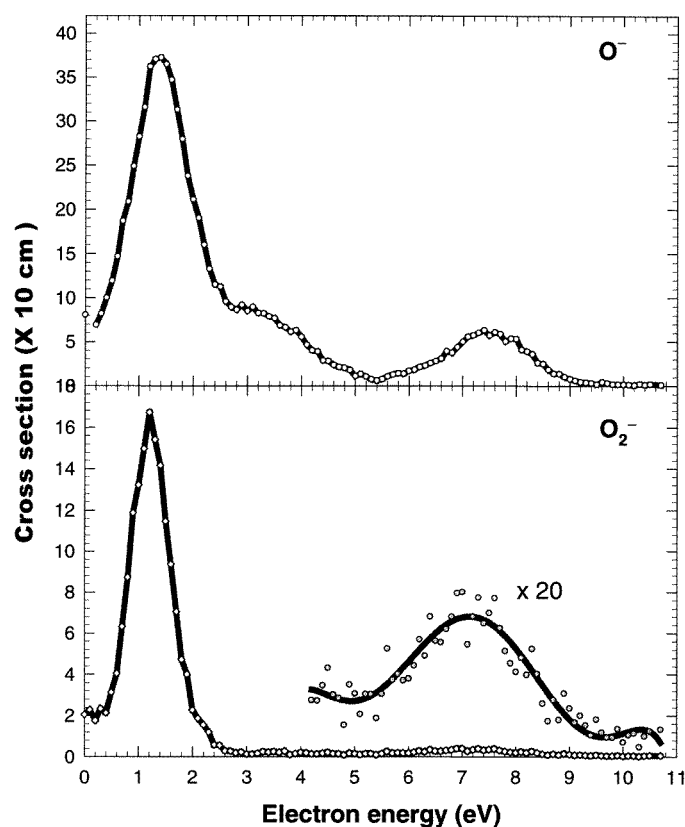


**Figure 2.** The cross section for the production of the  $O^-$  and the  $O_2^-$  ions from  $O_3$  as a function of the incident electron energy.

Skalny *et al*, the peak width is larger. The value measured in our experiment may also be about 10% lower than the true value, due to our relatively poor electron resolution. However, the energy integrated counts under the peak should remain the same. Our cross section for the first peak of  $O^-$  is  $3.7 \times 10^{-17} \text{ cm}^2$ , which is significantly higher than the  $2.8 \times 10^{-17} \text{ cm}^2$  of Skalny *et al* (1996). This may be due to the incomplete collection of high kinetic energy ions in their experiment as manifested by the absence of the shoulder at 3.0 eV in their data. It has been experimentally shown by Allan *et al* (1996a) that the kinetic energy of the  $O^-$  ions, at incident electron energy 1.3 eV, peaks at 0.1 eV, whereas that of the  $O^-$  ions at 3.2 eV incident electron energy, peaks at 2.1 eV. Our experiment was designed specifically to collect all the ions. Therefore, it is likely that the measured cross section at 1.4 eV for the  $O^-$  peak has an additional contribution from the shoulder at 3.0 eV, a contribution Skalny *et al* could not detect. This structure has been previously identified as a shape resonance with an  $A_1$  symmetry attributed to the negative-ion state by Allan *et al*. The overlap of this peak with the peak at 1.4 eV has the effect of enhancing the cross section and partially masking the form of the resonance peak responsible for the high kinetic energy fragments of  $O^-$ .

From figure 2 we observe that the low-energy peaks of  $O^-$  and  $O_2^-$  possibly share a common negative-ion resonant state. However, the  $O^-$  peak at these energies is significantly broader than the  $O_2^-$  peak. As mentioned earlier, Skalny *et al* (1996) and Allan *et al* (1996a) observed both the relative energy shift between the  $O^-$  and  $O_2^-$  peaks as well as the broader

**Table 1.** Summary of the experimental results obtained in the current experiment. The numbers in parentheses indicate the combined one-sigma error limits of the measurement.

| Electron energy (eV) | Feature       | O <sup>-</sup> cross section (10 <sup>-18</sup> cm <sup>2</sup> ) | O <sub>2</sub> <sup>-</sup> cross section (10 <sup>-18</sup> cm <sup>2</sup> ) |
|----------------------|---------------|---|--|
| 1.2                  | Peak          | —   | 16.8(±3.9)   |
| 1.4                  | Peak          | 37.0(±8.5)  | —  |
| 3.0                  | Shoulder      | 8.7   | —  |
| 6.5                  | Gradual slope | 3.0   | —  |
| 7.3                  | Peak          | —   | 0.4  |
| 7.5                  | Peak          | 6.0   | —  |

peak for the O<sup>-</sup>. An additional feature of the Allan *et al* measurement is a small, double-peak structure in O<sup>-</sup> at 1.18 and 1.35 eV. This structure was attributed to vibrational excitation of the neutral O<sub>2</sub> dissociation fragment. Furthermore, in an electron energy loss experiment, Allan *et al* (1996b) have shown that for incident electron energies higher than 1.2 eV there is an isotropic emission of electrons at the lower residual electron energies with pronounced vibrational structure. This fact was attributed to the autodetachment of electrons from the O<sub>2</sub><sup>-</sup> fragment in its ground and vibrationally excited states formed at these energies, illustrating a novel instance where both DEA and electron autodetachment from the fragment ion occur in rapid succession.

A recent experiment (Senn *et al* 1998) reported a narrow resonance feature in the O<sup>-</sup> yield from ozone at or close to zero energy. Some evidence for such a feature is also apparent in the total cross section measurements of Gulley *et al* (1998). Therefore, we performed a series of experiments at these very low energies by taking the negative-ion mass spectra over the range from 0 to 0.5 eV of electron energy in very small incremental steps (0.02 eV). The separate sets of measurements were necessitated by the drop in electron gun current at these energies and the energy calibration problems at these low energies. No resonance structure was seen close to 0 eV in our experiment in either the O<sup>-</sup> or O<sub>2</sub><sup>-</sup> ion peaks. However, this may be attributed to the inherent low resolution (from 400 to 500 meV) used in our experiments. Our relatively poor energy resolution would lead to a smearing out of this peak. One may argue that there may be a contribution due to this in the finite value of the cross section seen in O<sup>-</sup> at ~0 eV. However, we also see finite cross sections in the O<sub>2</sub><sup>-</sup> channel at ~0 eV. The reason for the finite cross section in both these channels at this energy, we believe, may be due to a convolution effect of the resonant peak with the tail of the electron energy distribution. The effect due to this would get amplified further due to the increase in path length at near zero energies as mentioned in the previous section.

From figure 2, it can be seen that there is a prominent resonance structure at about 7.5 eV in both the O<sup>-</sup> and O<sub>2</sub><sup>-</sup> channels. The O<sup>-</sup> cross section at this energy is of the same order as at 3.0 eV. The O<sub>2</sub><sup>-</sup> cross section at this energy is small and is found to be ~40 times smaller than the signal at 1.2 eV. We see some disagreement in the ratio of the relative cross section of the O<sub>2</sub><sup>-</sup> to O<sup>-</sup> at the 7.5 eV peak, with respect to the data reported by Walker *et al*. The measured ratio of Walker *et al* is a factor of two larger than that suggested by our data. However, in their experiment, Walker *et al* used a quadrupole mass spectrometer (QMS) for determining the ion counts as a function of mass to charge ( $m/e$ ). The transmission function of a QMS varies with  $m/e$  and is very sensitive to its tuning conditions. The TOF spectrometer used in our experiment is designed to collect all the ions independent of their kinetic energies, angular distributions and  $m/e$  ratios. The observed difference in the ratio of the O<sup>-</sup> to O<sub>2</sub><sup>-</sup> counts at 7.5 eV incident electron energy may be attributed to (a) possible discrimination for ions travelling along certain directions in their experiment and (b) unequal transmission

**Table 2.**  $O_3^-$  excited state calculations performed for the lowest energy states of the four symmetries exhibited by the  $C_{2v}$  molecules. Column 1 lists the symmetries in ascending order of vertical energies in the equilibrium configuration of the ground neutral state of  $O_3$  ( $X^1A_1$ ,  $d(O-O) = 1.27 \text{ \AA}$ ,  $\theta = 116.8^\circ$ ) and column 2 the energies. Column 3 lists the vertical energies of excitation from the ground  $O_3^-$  state ( $^2B_1$ ,  $d(O-O) = 1.35 \text{ \AA}$ ,  $\theta = 114.5^\circ$ ). Column 4 lists the calculations of Koch *et al* for comparison with our values in column 3.

| $O_3^-$ states | Vertical energy from<br>$O_3$ ( $X^1A_1$ ) (present calc.) | Vertical energy from<br>$O_3^-$ ( $X^2B_1$ ) (present calc.) | Vertical energy from<br>$O_3^-$ ( $X^2B_1$ ) (Koch <i>et al</i> 1993) |
|----------------|--|--|---|
| $^2B_1$        | -2.01 eV   | 0.00 eV  | 0.00 eV   |
| $^2A_1$        | +0.75 eV   | +2.38 eV   | +2.28 eV  |
| $^2B_2$        | +0.94 eV   | +2.25 eV   | +2.26 eV  |
| $^2A_2$        | +1.58 eV   | +2.87 eV   | +2.85 eV  |

efficiencies for the different ions in the QMS, as has been pointed out by Walker *et al*. It is possible that more than one resonance is responsible for DEA at these energies. This can be seen from the shape of the peak in the  $O^-$  data, which has a pronounced asymmetry. Allan *et al* (1996a) saw the signature of a resonance at 6.6 eV in their scattering experiments. They do not report any DEA structure at this energy though they mention having seen a DEA structure at 7.5 eV. The kinetic energy of these ions in their experiment was observed to be between 1 and 2 eV. The negative-ion state(s) responsible for  $O^-$  and  $O_2^-$  ions are again likely to be the same, because of the similarity of the energy at which these peaks are seen.

To facilitate the interpretation of the experimental results, quantum chemical calculations have been performed using the Gaussian 94 package, at the Quadratic CI (single and doubles) level with the Dunning's aug-cc-pVDZ basis set so that d orbitals, polarization and diffuse functions are included. The diffuse functions are particularly important as the calculations are performed for negative ions. Due to the limitation of the method, we had to restrict our calculations to the ground state of  $O_3^-$  and the lowest states of different symmetries. We determined the vertical energies from the ground neutral equilibrium configuration, to the lowest negative-ion states of  $O_3^-$  of different symmetries. The ground neutral state is  $^1A_1$  and its equilibrium structure is  $d(O-O) = 1.27 \text{ \AA}$ ,  $\theta = 116.8^\circ$ . Since the negative-ion precursor formed by electron attachment is well described by the Franck-Condon principle of vertical transitions, the vertical transition energies for the negative-ion states were calculated from the neutral ground state in its equilibrium geometry. Calculations were also performed for the vertical transition energies from the  $X^2B_1$  negative-ion state, to check present calculations with those in the literature (Koch *et al* 1993), and against the experimental data on photodetachment and the electron affinity. The results of these calculations are summarized in table 2. Good agreement is found with Koch *et al*. Our calculated value for the electron affinity is 2.318 eV, which is only 10% more than the experimental value, i.e. 2.103 eV, obtained by Novick *et al* (1979).

From table 2, it is clear that the negative-ion ground state  $^2B_1$  cannot be accessed by electron capture as it is energetically lower than the ground neutral state. The three remaining negative-ion states of different symmetries, in increasing order of their vertical energies from the electronic ground state of the neutral  $O_3$  ( $X^1A_1$ ), are the  $^2A_1$ ,  $^2B_2$  and  $^2A_2$  states.

Based on the selection rules for the electron capture (Krishnakumar *et al* 1996), the negative-ion states that could be accessed from the ground state of  $O_3$  with  $A_1$  symmetry are  $A_1$ ,  $B_1$  and  $B_2$ . The only route by which the  $^2A_2$  state can be produced by electron capture to the ground neutral state is if the neutral molecule is in its asymmetric stretch vibrational mode with  $C_s$  symmetry. We do not expect this mode to be populated to any significant extent



and hence rule out the possibility of attachment to the  $^2A_2$  state. This is also in agreement with the assignments of the negative-ion symmetries by Allan *et al* (1996a) and they do not attribute any of the experimentally observed resonances to the  $A_2$  state. Hence, either the  $^2A_1$  or the  $^2B_2$  might be candidates for the DEA peak structure observed at  $\sim 1.4$  eV. However, since our computed energy values differ by 0.5 eV from the experimental values of energy, it is not possible to make a definite assignment of the dissociating negative-ion state. It must be added that the calculations presented here, though reliable, are used in the spirit of a guide to the physics rather than as accurate theoretical numbers about which to look for experimental signatures, since besides the four states listed in the table, there could be others at these energies which are computationally inaccessible to the methodology employed.

Measurements by Allan *et al* (1996a) show a small peak at 0.1 and 0.4 eV in the  $O^-$  ion. These peaks manifest themselves as a structure on the 1.3 eV peak of their experiment. No structure was seen in the  $O_2^-$  peak. Allan *et al* (1996a) suggest that this peak may be due to the high-lying tail of the ground negative-ion state, i.e.  $X^2B_1$ . We could not detect any structure at these energies. The probable reason for this may be our relatively poor electron energy resolution, as compared with that of Allan *et al* (1996a). The resonance feature reported at 0.4 eV is narrow, has a substantially lower cross section than the 1.4 eV peak and it also overlaps with this peak. Due to the poor electron energy resolution in our experiment, the 0.4 eV peak is possibly being smeared out. It is interesting to note that the experiment of Walker *et al* (1996), with similar energy resolution as our measurements, also failed to detect this feature. Our calculations show that the negative-ion ground state is well below ( $\sim 2.0$  eV) the ground neutral state, i.e.  $^1A_1$ , in its equilibrium configuration. Thus, it is likely that the 0.4 eV resonance structure does not originate from electron capture to the ground negative-ion state even in its high-lying tail region, as proposed by Allan *et al* (1996a).

## Conclusions

In conclusion, in this paper we report the DEA cross sections for  $O_3$  in the energy range from 0 to 10 eV. The qualitative features of our data compare well with previous work on electron scattering as well as DEA studies. The  $O^-$  ion cross section peak occurs at 1.4 eV and is  $3.7(\pm 0.85) \times 10^{-17} \text{ cm}^2$ . The  $O_2^-$  cross section peak at 1.2 eV is  $1.68(\pm 0.39) \times 10^{-17} \text{ cm}^2$ . Quantum chemical calculations show that several low-lying candidate states exist for DEA and that the peak at 0.4 eV seen in the  $O^-$  data in the experiment of Allan *et al* (1996a), may not be due to the high-energy tail of the  $^2B_1$  ground negative-ion state as has been proposed.

## Acknowledgments

NJM wishes to thank the Royal Society and EPSRC for support.

## References

- Allan M, Asmis K R, Popovic D B, Stepanovic M, Mason N J and Davies J A 1996a *J. Phys. B: At. Mol. Opt. Phys.* **29** 4727
- 1996b *J. Phys. B: At. Mol. Opt. Phys.* **29** 3487
- Curran R K 1961 *J. Chem. Phys.* **35** 1849
- Frisch M J *et al* 1995 *Gaussian 94* Revision C.2 (Pittsburgh, PA: Gaussian, Inc.)
- Gulley R J, Field T A, Steer W A, Mason N J, Lunt S L, Ziesel J-P and Field D 1998 *J. Phys. B: At. Mol. Opt. Phys.* **31** 5197
- Kieffer L J and Dunn G H 1966 *Rev. Mod. Phys.* **38** 1
- Koch W, Frenking G, Steffen G, Reinen D, Jansen M and Assenmacher W 1993 *J. Chem. Phys.* **99** 1271

- Krishnakumar E, Kumar S V K, Rangwala S A and Mitra S K 1996 *J. Phys. B: At. Mol. Opt. Phys.* **29** L65  
——— 1997 *Phys. Rev. A* **56** 1945  
Krishnakumar E and Nagesha K 1992 *J. Phys. B: At. Mol. Opt. Phys.* **25** 1645  
Krishnakumar E and Srivastava S K 1992 *Int. J. Mass. Spectrom. Ion Processes* **113** 1  
——— 1994 *J. Phys. B: At. Mol. Opt. Phys.* **27** L 251  
Kumar S V K, Ananthakrishnan T S, Krishnakumar E and Rangwala S A 1997 *Proc. 20th Int. Conf. on Physics of Electronic and Atomic Collisions* ed F Aumayr, G Betz and H P Winter (Singapore: World Scientific) FR201  
Newson K A, Luc S M, Price S D and Mason N J 1995 *Int. J. Mass. Spectrom. Ion Processes* **148** 203  
Novick S E, Engelking P C, Jones P L, Futrell J H and Lineberger W C 1979 *J. Chem. Phys.* **70** 2652  
Rapp D and Briglia D D 1965 *J. Chem. Phys.* **43** 4183  
Senn G, Skalny J D, Stamatovic A, Mason N J and Märk T D 1999 *Phys. Rev. Lett.* **85** 5308  
Skalny J D, Matejcik S, Kiendler A, Stamatovic A and Märk T D 1996 *Chem. Phys. Lett.* **255** 11  
Stelman D, Moruzzi J L and Phelps A V 1972 *J. Chem. Phys.* **56** 4183  
Walker I C, Gingell J M, Mason N J and Marston G 1996 *J. Phys. B: At. Mol. Opt. Phys.* **29** 4749  
van Zyl B and Stephen T M 1994 *Phys. Rev. A* **50** 3164